Center for Turbulence Research
Proceedings of the Summer Program 2008

Numerical description of dilute particle-laden flows by a quadrature-based moment method

By N. Le Lostec†, R. O. Fox‡, O. Simonin¶ AND P. Villedieu†

The numerical simulation of gas-particle flows is divided into two families of methods. In Euler-Lagrange methods individual particle trajectories are computed, whereas in Euler-Euler methods particles are characterized by statistical descriptors. Lagrangian methods are very precise but their computational cost increases with instationarity and particle volume fraction. In Eulerian methods (also called moment methods) the particle-phase computational cost is comparable to that of the fluid phase but requires strong simplifications. Existing Eulerian models consider unimodal or close-to-equilibrium particle velocity distributions and then fail when the actual distribution is far from equilibrium. Quadrature-based Eulerian methods introduce a new reconstruction of the velocity distribution, written as a sum of delta functions in phase space constrained to give the right values for selected low-order moments. Two of these quadrature-based Eulerian methods, differing by their reconstruction algorithm, are the focus of this work. Computational results for two academic cases (crossing jets, Taylor-Green flow) are compared to those of a Lagrangian method (considered as the reference solution) and of an existing second-order moment method. With the quadrature-based Eulerian methods, significant qualitative improvement is noticed compared to the second-order moment method in the two test cases.

1. Introduction

1.1. *Overview*

1.1.1. *Physics of fluid-particle flows*

Rarefied gaseous flows can be parameterized by the Knudsen number, which is the ratio of the mean free path to the characteristic length of the system (Chapman & Cowling 1970). Low Knudsen means that the kinetic descriptor – the velocity distribution function – is close to the equilibrium distribution (Maxwellian) because the collisions redistribute the particles' velocities over the local Maxwellian distribution. For large Knudsen, particles travel over a long distance between collisions and thus the local velocity distribution function can be far from equilibrium. But even for small Knudsen, locally one can have a non-equilibrium distribution. For example, close to a wall the particle velocity distribution function has no reason to be Maxwellian since there are two populations of particles: those moving toward the wall and those coming from the wall after rebound.

For fluid-particle flows more physical processes should be considered: fluid-particle interactions, particle evaporation, coalescence and breakage. Note that the fluid flow is turbulent in general. Considering only the velocities, two dimensionless numbers can be introduced: the Reynolds number characterizing the fluid-particle drag and the Stokes

† Office National d'Etudes et de Recherches Aérospatiales, France
‡ Department of Chemical and Biological Engineering, Iowa State University
¶ Institut de Mécanique des Fluides de Toulouse, France

number characterizing the particle dynamic response time relative to the fluid time scale. The Stokes number is thus an indicator of how close the particle velocity is to the fluid velocity. For small Stokes, particles will have the same velocity as the fluid. For large Stokes, the particle velocity will be less influenced by the fluid and thus remains sensitive to the particle inertia. Hence, at a given location, for finite Stokes number, particles will possibly have different velocities, and particle trajectory crossing will occur, resulting in a non-Maxwellian distribution function. In the large inertia limit ($\mathrm{St} \to \infty$), particle motion is stochastically equivalent to Brownian motion. As particle barely see the fluid, their velocity results of the interaction with remote fluid velocity. Because locally particles come from different remote regions, which fluid velocities are not correlated, particle velocities are not correlated and the velocity distribution function is Maxwellian (Fevrier, Simonin & Squires 2005).

1.1.2. *Numerical simulation of fluid-particle flows*

Existing moment methods assume either an unimodal or a close-to-Maxwellian velocity distribution function. The first class of methods (unimodal) does not account for particle trajectory crossing and is unable to describe precisely phenomena such as clustering, aggregation or breakage. The second (close-to-equilibrium) is valid only when the velocity distribution is close to equilibrium and thus fails to describe dilute flows of large particles as reported in Sakiz & Simonin 1999. Lagrangian methods can handle both particle trajectory crossing and non-equilibrium velocity distribution, but the huge number of particles needed to reduce the statistical noise in Eulerian statistics leads to significantly large computational costs. Because of the orders-of-magnitude difference between the computational costs of Eulerian and Lagrangian approaches, an Eulerian method that could accurately address particle trajectory crossing would be a good basis for the integration of effects such as aggregation and breakage into a reduced-cost calculation code. In this work, we focus on the treatment of particle velocity and leave aside evaporation, coalescence and polydispersity. Therefore only transport, drag and particle collisions remain.

While in Lagrangian simulations the trajectory of each particle is computed, the Eulerian approach characterizes the particles on a statistical basis. The kinetic equation gives the evolution of the velocity distribution function whose moments are the desired macroscopic quantities. The kinetic equation is not solved directly (i.e., the moments are calculated), but it is the underlying fundamental equation containing the physics. The main difficulty is that the transport equation for a given moment involves higher-order moments. Considering that only a finite set of moments is calculated, closures have to be made for the non-calculated moments. One way to obtain these closures is to make assumptions about the velocity distribution function. Existing model assumptions include delta-shaped function or close-to-Maxwellian distribution, but these cannot describe far-from-equilibrium distributions. In contrast, the quadrature method of moments (QMOM) introduces quadrature-based closures, and previous work has shown it is able to handle particle trajectory crossing (Desjardins, Fox & Villedieu 2008).

1.2. *Objective*

The global objective of this work is to evaluate the ability of quadrature-based moment methods to describe fluid-particle flows. Two quadrature methods are considered, each based on the same 1-D quadrature algorithm, but coupled differently to construct the final 2-D quadrature. Computational results for the quadrature-based moment closures in two academic cases are compared to reference solutions generated by a Lagrangian code

(with a Babovsky algorithm for Monte-Carlo collisions, see Babovsky 1986 and Nanbu 1980) and the results of an existing second-order moment method. The latter comparison allows us to estimate the possible qualitative enhancement due to the quadrature-based methods.

The test cases include transport of particles, one-way fluid-particle interactions (drag) and particle-particle collisions. The physical-space dimension is restricted to two as one of the quadrature methods has been developed and implemented only for one and two dimensions. In the first test case, a collisional regime in the presence of particle trajectory crossing without drag is explored. The chosen flow geometry is the crossing of two particle jets. The second test case focuses on the interaction of the inertial regime with transport, with particles evolving in a Taylor-Green flow without collisions.

2. Moment method

2.1. *Kinetic description*

The kinetic descriptor is the velocity distribution function f, which is the particle number density in phase space (positions-$\vec{x} \otimes$ velocities-$\vec{v}$). Its transport equation is a Boltzmann-like equation:

$$\frac{\partial f(t,\mathbf{x},\mathbf{v})}{\partial t} + \mathbf{v} \cdot \mathbf{grad}_{\mathbf{x}}\ f(t,\mathbf{x},\mathbf{v}) + div_v(f(t,\mathbf{x},\mathbf{v})\ \mathbf{a}) = \left.\frac{\partial f(t,\mathbf{x},\mathbf{v})}{\partial t}\right|_{coll}$$

where $\mathbf{a}$ is the acceleration the particles experience (we will provide its expression later). On the r.h.s. is the collision term, which is the variation of the velocity distribution function due to collisions. The Eulerian (macroscopic) descriptors are the moments of the velocity distribution function, defined, for a 1-D velocity space, as

$$M^q = \int v^q f(t,\mathbf{x},\mathbf{v})\,\mathrm{d}\mathbf{v} \quad \begin{cases} q = 0, \text{particle number density } (n), \\ q = 1, n \text{ times particle mean velocity}, \\ q = 2, n \text{ times particle mean square velocity}. \end{cases}$$

Eulerian methods solve transport equations for such moments.

2.2. *Moment transport equations*

The moment transport equations come from integrating over velocity space the kinetic equation multiplied by powers of the velocities components, denoted ψ. Its general form is

$$\frac{\partial}{\partial t}\left[\int \psi f\,\mathrm{d}\mathbf{v}\right] + \frac{\partial}{\partial x_i}\left[\int v_i \psi f\,\mathrm{d}\mathbf{v}\right] = \int a_i \frac{\partial \psi}{\partial v_i} f\,\mathrm{d}\mathbf{v} + \mathbf{C}(\psi)$$

where the collision terms are defined as

$$\mathbf{C}(\psi) = \int \psi \left.\frac{\partial f(t,\mathbf{x},\mathbf{v})}{\partial t}\right|_{coll} \mathrm{d}\mathbf{v}.$$

Note that the moment transport equations can be written for either the moments or the central moments corresponding to integral of total velocity $\mathbf{v}$ or velocity fluctuation $\mathbf{v}' = \mathbf{v} - \mathbf{U}$ with respect to the mean velocity $\mathbf{U} = \frac{1}{n}\int \mathbf{v} f\,\mathrm{d}\mathbf{v}$. The equations for moments and central moments are strictly equivalent. Any total moment can be expressed in terms of lower order central moments.

2.3. *Models for collisions and acceleration*

The collision term can be closed using its complete expression given by Boltzmann, for all moment methods considered in this paper. But, for simplification, and without loss of generality, we close it using a relaxation-time approximation model (also called BGK model, see Bhatnagar, Gross & Krook 1954):

$$\left.\frac{\partial f(t,\mathbf{x},\mathbf{v})}{\partial t}\right|_{coll} = \frac{f_{\mathrm{eq}} - f}{\tau_{\mathrm{coll}}}$$

where f_{eq} is the equilibrium velocity distribution function and τ_{coll} the characteristic relaxation time, taken equal to the mean time between collisions. Then, as the expression for f_{eq} is known:

$$f_{\mathrm{eq}} = \frac{n}{(2\pi\sigma)^{D/2}} \exp\left(-\mathbf{v}'^2/2\sigma\right)$$

where D is the dimension of phase space and $\sigma = D^{-1}\sum_i \int v_i' v_i' f \,\mathrm{d}\mathbf{v}$, the collision terms are directly functions of the moments.

The acceleration has two contributions: drag and gravity. The model for drag acceleration is the Stokes drag with fixed dynamic response time. Thus, $\mathbf{a} = \mathbf{g} + {\tau_p}^{-1}(\mathbf{V_f} - \mathbf{v})$ where $\tau_p = 2\rho_p r^2/(9\mu_f)$, $\mathbf{V_f}$ is the local fluid velocity, $\mathbf{v}$ the particle velocity, ρ_p the particle mass density, r the particle radius, and μ_f the fluid dynamic viscosity.

2.4. *2-D moment equations*

Considering the general moment transport equation given above, in two dimensions and for moments up to third order ($\psi = \{1, v_i, v_i v_j, v_i v_j v_k\}$), the 2-D moment equations are

$$\frac{\partial M^0}{\partial t} + \frac{\partial M_i^1}{\partial x_i} = 0,\ \frac{\partial M_i^1}{\partial t} + \frac{\partial M_{ij}^2}{\partial x_j} = A_i^1,$$
$$\frac{\partial M_{ij}^2}{\partial t} + \frac{\partial M_{ijk}^3}{\partial x_k} = A_{ij}^2 + \mathbf{C}(v_i v_j),\ \frac{\partial M_{ijk}^3}{\partial t} + \frac{\partial M_{ijkl}^4}{\partial x_l} = A_{ijk}^3 + \mathbf{C}(v_i v_j v_k),$$

where acceleration terms A_i^1, A_{ij}^2, A_{ijk}^3 and collision terms $\mathbf{C}(v_i v_j)$, $\mathbf{C}(v_i v_j v_k)$ can be expressed in terms of the moments up to third order (i.e., they are closed).

3. Eulerian gradient-diffusion model

3.1. *Existing kinetic theory based moment methods*

The existing Eulerian methods developped in the frame of classical kinetic theory of gases are using transport equations for central velocity moments:

$$R_{ij} = \frac{1}{n}\int v_i' v_j' f \,\mathrm{d}\mathbf{v},\ S_{ijk} = \frac{1}{n}\int v_i' v_j' v_k' f \,\mathrm{d}\mathbf{v},\ Q_{ijkl} = \frac{1}{n}\int v_i' v_j' v_k' v_l' \,\mathrm{d}\mathbf{v}.$$

An Eulerian model is characterized by its order, which corresponds to the maximum order of the transported moments:

- first-order model – n (number density) and U_i (mean velocity) are transported (equivalent to pressure-less gas dynamics),
- Reduced second-order model – n, U_i and $\sum_i R_{ii}$ (kinetic energy) are transported (equivalent to Navier-Stokes equation),

• Full second-order model – n, U_i, R_{ij} (kinetic stresses) are transported (equivalent to Grad's moment method for rarefied gases).

The most basic Eulerian model (first-order model) assumes that the velocity distribution function is a mean-velocity Dirac: $f = n\,\delta\,(\mathbf{v} - \mathbf{U})$. Thus all particles at the same location have the same velocity, equal to the mean velocity of all the particles arriving at that location. For this reason, it is also referred to as the "sticky-particle" model.

For existing Eulerian models of second or higher order, the velocity distribution is assumed to be close to an equilibrium distribution corresponding to the local Maxwellian. Then, Enskog's or Grad's method may be used to close the collision terms and derive gradient-diffusion model for the unknown higher order moments appearing in the computed transport equations.

3.2. *Full second-order model*

Here we present the full second-order Eulerian model of Simonin 1991, called particle kinetic stress transport model (see also He & Simonin 1993), which we use for comparison with quadrature-based models. In the original work, considering a three-dimensional space, the collision terms are closed using a presumed velocity distribution function f_{coll} based on a third-order Grad's expansion around the equilibrium distribution function f_{eq}: $f_{\text{coll}} = P_3(\mathbf{v}) f_{\text{eq}}$ where $P_3(\mathbf{v})$ is a third-order polynomial of velocities whose coefficients are expressed as functions of the transported moments and such that f_{coll} gives the right values of the moments up to S_{ijk}. Here we use a BGK model for the collision terms so we do not need the Grad's expansion, and model is developed in two dimensions. The value of the triple correlation S_{ijk} appearing in the transport equation of R_{ij} comes from simplifying the transport equation for S_{ijk} using the following assumptions:

• equilibrium reached – temporal variation and convection term equals to zero,

• quadruple velocity correlation Q_{ijkl} takes the value it would have for an anisotropic Gaussian velocity distribution function,

• production terms by the mean velocity gradients are neglected,

The resulting gradient-diffusion closure expression for S_{ijk} is

$$S_{ijk} = -K_{ip}\frac{\partial}{\partial x_p}R_{jk} - K_{jp}\frac{\partial}{\partial x_p}R_{ki} - K_{kp}\frac{\partial}{\partial x_p}R_{ij}$$

where $K_{pq} = (3/\tau_p + 1/\tau_{\text{coll}})^{-1} R_{pq}$.

4. 2-D quadrature-based moment method

As we used the same models for collisions and acceleration as in the full second-order model, and because these models lead to terms that are already in closed form, the only difference between the full second-order model and the quadrature-based moment method resides in the closure of the third-order moments. In the quadrature-based method, we solve the third-order moment transport equation and use quadrature to compute its fluxes (i.e., the fourth-order moments). Thus, these two methods are not exactly of the same order. For the quadrature-based moment method we consider the ten 2-D moments up to third order:

$$W^2 = (M^0, M_1^1, M_2^1, M_{11}^2, M_{12}^2, M_{22}^2, M_{111}^3, M_{112}^3, M_{122}^3, M_{222}^3).$$

where

$$M^0 = \int f(t,\mathbf{x},\mathbf{v})\,\mathrm{d}\mathbf{v}, \quad M_i^1 = \int v_i\ f(t,\mathbf{x},\mathbf{v})\,\mathrm{d}\mathbf{v}$$
$$M_{ij}^2 = \int v_i v_j\ f(t,\mathbf{x},\mathbf{v})\,\mathrm{d}\mathbf{v}, \quad M_{ijk}^3 = \int v_i v_j v_k\ f(t,\mathbf{x},\mathbf{v})\,\mathrm{d}\mathbf{v}$$

4.1. *Quadrature closure*

In quadrature-based closures, the particle velocity distribution function f is reconstructed from the moments in the form

$$f(\mathbf{v}) = \sum_{\alpha=1}^{N} n_\alpha \delta(\mathbf{v} - \mathbf{U}_\alpha)$$

where $n_\alpha(\mathbf{x},t)$ are non-negative weights and $\mathbf{U}_\alpha(\mathbf{x},t)$ are the velocity abscissas. Let $V^4 = [(n_\alpha, \mathbf{U}_\alpha)]$ with $\alpha \in (1,\ldots,4)$ denote the set of weights and abscissas for the 4-node quadrature reconstruction of f. Note that the set of quadrature nodes V^4 contains 12 unknowns (i.e., four weights and four two-component velocity vectors). To find the components of V^4, we work with the velocity moments up to third order, which are related to the quadrature weights and abscissas by

$$M^0 = \sum_{\alpha=1}^{4} n_\alpha,\ M_i^1 = \sum_{\alpha=1}^{4} n_\alpha U_{\alpha i},\ M_{ij}^2 = \sum_{\alpha=1}^{4} n_\alpha U_{\alpha i} U_{\alpha j},\ M_{ijk}^3 = \sum_{\alpha=1}^{4} n_\alpha U_{\alpha i} U_{\alpha j} U_{\alpha k}. \tag{4.1}$$

Quadrature inversion is the algorithm for computing V^4 from W^2. The inverse operation (finding W^2 from V^4) is given in Eq. (4.1), which we refer to as *projection*. In general, it will not be possible to represent all possible moment sets in W^2 using weights and abscissas in V^4. We will therefore define the set of quadrature-representable moments as $W^{2\dagger} \subset W^2$.

4.2. *Inversion by frame change*

Following the work of Fox 2008, the frame change inversion algorithm consists in defining a linear transformation $\mathbf{A}$ that diagonalize the particle velocity covariance matrix $\mathbf{R} = [R_{ij}]$, based on its Cholesky decomposition. Then, we introduce a transformed velocity vector $\mathbf{X} = [X_1\ X_2]^{\mathrm{T}}$ defined by

$$\mathbf{X} = \mathbf{A}^{-1}(\mathbf{v} - \mathbf{U}) \quad \text{so that} \quad \mathbf{v} = \mathbf{A}\mathbf{X} + \mathbf{U}.$$

We introduce the first four moments of X_i by $m_i^k,\ k \in (0,1,2,3)$. They are related to the velocity moments by

$$m_i^0 = 1,\ m_i^1 = 0,\ m_i^2 = 1,\ m_i^3 = h_i\left(\mathbf{A}, \mathbf{U}, M_{111}^3/M^0, \ldots, M_{222}^3/M^0\right),$$

where h_i depends, in general, on all ten moments in W^2. In other words, $W^{2\dagger}$ is an 8-D linear subspace of W^2 defined *locally* using $\mathbf{A}$.

In order to compute V^4, we will use a tensor product in the transformed velocity space: from two two-node one-dimension quadratures we build a four-node two-dimension quadrature. Using two-node quadrature (McGraw 1997) for each $i \in (1,2)$, the moments of X_i can be inverted to find $(n_{(1)}, n_{(2)}, X_{(1)}, X_{(2)})_i$:

$$n_{(i)1} = 0.5 + \gamma_i,\ X_{(i)1} = -\left(\frac{1-2\gamma_i}{1+2\gamma_i}\right)^{1/2},\ n_{(i)2} = 0.5 - \gamma_i,\ X_{(i)2} = \left(\frac{1+2\gamma_i}{1-2\gamma_i}\right)^{1/2},$$

where $(-1/2 < \gamma_i < 1/2)$

$$\gamma_i = \frac{m_i^3/2}{[(m_i^3)^2 + 4]^{1/2}}.$$

Note that for a joint Gaussian distribution $\gamma_i = 0$. In the original velocity space, the four-node quadrature approximation is then defined as

$$V^4 = [(n_1, \mathbf{A}[X_{(1)1}\ X_{(2)1}]^{\mathrm{T}} + \mathbf{U}),\ (n_2, \mathbf{A}[X_{(1)1}\ X_{(2)2}]^{\mathrm{T}} + \mathbf{U}),$$
$$(n_3, \mathbf{A}[X_{(1)2}\ X_{(2)1}]^{\mathrm{T}} + \mathbf{U}),\ (n_4, \mathbf{A}[X_{(1)2}\ X_{(2)2}]^{\mathrm{T}} + \mathbf{U})]$$

where

$$n_1 = M^0(0.5 + \gamma_1)(0.5 + \gamma_2), \quad n_2 = M^0(0.5 + \gamma_1)(0.5 - \gamma_2),$$
$$n_3 = M^0(0.5 - \gamma_1)(0.5 + \gamma_2), \quad n_4 = M^0(0.5 - \gamma_1)(0.5 - \gamma_2).$$

Note that these weights are always non-negative. At any point in the solution procedure for solving the ten moment equations, the moments in W^2 can be projected into $W^{2\dagger}$ using the weights and abscissas (e.g., Eq (4.1)).

4.3. *Direct inversion*

The principle behind direct inversion is to compute two 1-D quadratures and to couple them, with respect to particle velocity covariance, to form a 2-D quadrature. We start by defining the 8-D moment subspace of W^2 by

$$W^{2\prime} = (M^0, M_1^1, M_2^1, M_{11}^2, M_{12}^2, M_{22}^2, M_{111}^3, M_{222}^3),$$

and two subsets of moments:

$$W_1^1 = (M^0, M_1^1, M_{11}^2, M_{111}^3) \text{ and } W_2^1 = (M^0, M_2^1, M_{22}^2, M_{222}^3).$$

Each W^1 subset yields a two-node 1-D quadrature approximation:

$$V_1^2 = [(\alpha_1, X_{(1)1}), (\alpha_2, X_{(1)2})] \text{ and } V_2^2 = [(\beta_1, X_{(2)1}), (\beta_2, X_{(2)2})].$$

The 2-D quadrature discrete velocities are those of the 1-D quadrature, combined using a tensor-product so that we have only two discrete velocities per direction but four velocity vectors:

$$\mathbf{U}_1 = \begin{pmatrix} X_{(1)1} \\ X_{(2)1} \end{pmatrix},\ \mathbf{U}_2 = \begin{pmatrix} X_{(1)1} \\ X_{(2)2} \end{pmatrix},\ \mathbf{U}_3 = \begin{pmatrix} X_{(1)2} \\ X_{(2)1} \end{pmatrix},\ \mathbf{U}_4 = \begin{pmatrix} X_{(1)2} \\ X_{(2)2} \end{pmatrix}.$$

The coupling is done by computing the weights from the 1-D quadrature weights α_i and β_i that yield the correct value of the second-order cross-moment M_{12}^2. In this case off-diagonal third order moments M_{122}^3 and M_{112}^3 are not used. Defining $\rho = R_{12}/\sqrt{R_{11}R_{22}}$, a straightforward computation gives the 2-D quadrature weights:

$$n_1 = \left(\rho + \sqrt{\frac{\alpha_1\beta_1}{\alpha_2\beta_2}}\right)\frac{\sqrt{\alpha_1\alpha_2\beta_1\beta_2}}{M^0},\ n_2 = \left(-\rho + \sqrt{\frac{\alpha_1\beta_2}{\alpha_2\beta_1}}\right)\frac{\sqrt{\alpha_1\alpha_2\beta_1\beta_2}}{M^0},$$
$$n_3 = \left(-\rho + \sqrt{\frac{\alpha_2\beta_1}{\alpha_1\beta_2}}\right)\frac{\sqrt{\alpha_1\alpha_2\beta_1\beta_2}}{M^0},\ n_4 = \left(\rho + \sqrt{\frac{\alpha_2\beta_2}{\alpha_1\beta_1}}\right)\frac{\sqrt{\alpha_1\alpha_2\beta_1\beta_2}}{M^0}.$$

Then the four-node quadrature approximation is defined as

$$V^4 = [(n_1, \mathbf{U}_1), (n_2, \mathbf{U}_2), (n_3, \mathbf{U}_3), (n_4, \mathbf{U}_4)].$$

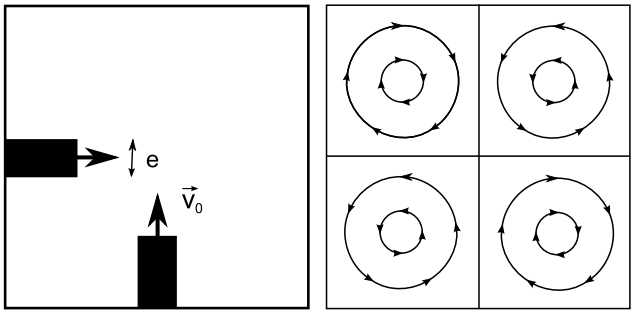

FIGURE 1. Schematics showing the two test cases. Left: crossing jets. Right: Taylor-Green flow.

This moment-inversion method does not ensure positive weights. Thus, if one weight happens to be negative, we change the value of the third-order moments to set the weight equal to zero, and recompute the other weights.

5. Flow configurations and results

The quadrature method involving frame change is referred to as QMOM #1 and the direct inversion method as QMOM #2. Here, we compare simulation results for the two test cases presented in Fig. 1.

5.1. *Crossing jets*

The physical processes modeled in the crossing-jets test case are transport and collision. The objective is to explore different collisional regimes, characterized by different Knudsen numbers. In the kinetic theory of gases, the Knudsen number is defined as the ratio of the mean free path to the characteristic length of the system. It can also be seen as the ratio of the collision time τ_{coll} to the convection time τ_{conv}:

$$\text{Kn} = \frac{\tau_{\text{coll}}}{\tau_{\text{conv}}}$$

The expression for the collision time is taken from the kinetic theory: $\tau_{\text{coll}} = 1/2nd_p\sqrt{R_{ii}}$, where n is the local particle number density, d_p the particle's diameter, R_{ii} the mean square fluctuating velocity, and the convection time is the time for one jet to cross the other: $\tau_{\text{conv}} = e/v_0$, e being the jet width and v_0 the jet velocity before crossing. Considering two jets of equal density and velocity magnitude (Fig. 1), the Knudsen number becomes

$$\text{Kn} = \frac{1}{4ned_p\sqrt{2}}$$

where n is the particle number density of the jets before collision.

Figures 2–4 show the results for Knudsen numbers 0.1, 1 and 5, respectively. The computed domain size is 1×1 m^2, the jet width is $e = 0.1$ m and the inlet jet velocity is $v_0 = 1$ m/s. For the most collisional case ($Kn = 0.1$ in Fig. 2), the full second-order model, compared to the Lagrangian reference, spreads the particles too much but the agreement is satisfactory. The two impinging jets join in a mean jet toward the diagonal. The results for the quadrature methods are quite different from the Lagrangian method. There is accumulation of particles close to the crossing, and parts of the jets are deflected away by a small angle after the crossing region. No mean jet is produced.

In the intermediate collisional regime ($Kn = 1$ in Fig. 3), the Lagrangian result shows

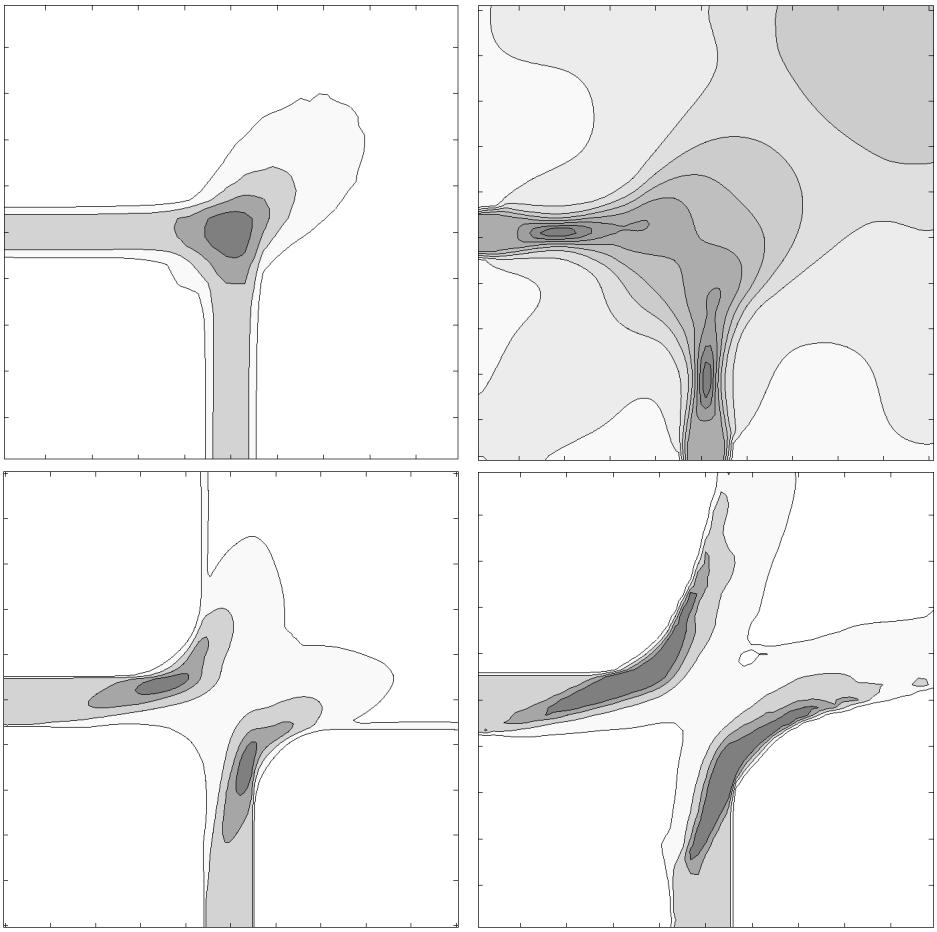

FIGURE 2. Particles' number density map and isocontours for crossing jets with $Kn = 0.1$. Density proportional to darkness. Domain size: 1 m $\times$1 m. Top left: Lagrangian. Top right: full second-order model. Bottom left: QMOM #1. Bottom right: QMOM #2.

that the jets cross and barely see each other. In contrast, the full second-order model predicts a mean jet directed toward the diagonal with a $\pi/2$ spreading angle. Some particles are also diffused toward the diagonal but in the opposite direction of the mean jet. The quadrature methods allow the jets to cross but, surprisingly, with post-crossing jets slightly deflected in the direction opposite of the mean jet, and excessive spread for QMOM #1. QMOM #2 also produces a narrow reverse-diffused jet. Neither the results of the second-order model nor the quadrature methods agree well with the Lagrangian method. However, only the quadrature methods allow part of the jets to cross.

In the least collisional case ($Kn = 5$ in Fig. 4), the jets cross without noticeable collisions with the Lagrangian method. Results of the quadrature methods show that the post-crossing jets are disturbed, slightly for QMOM #2, significantly for QMOM #1. As noted earlier, the second-order model performs poorly for large Kn.

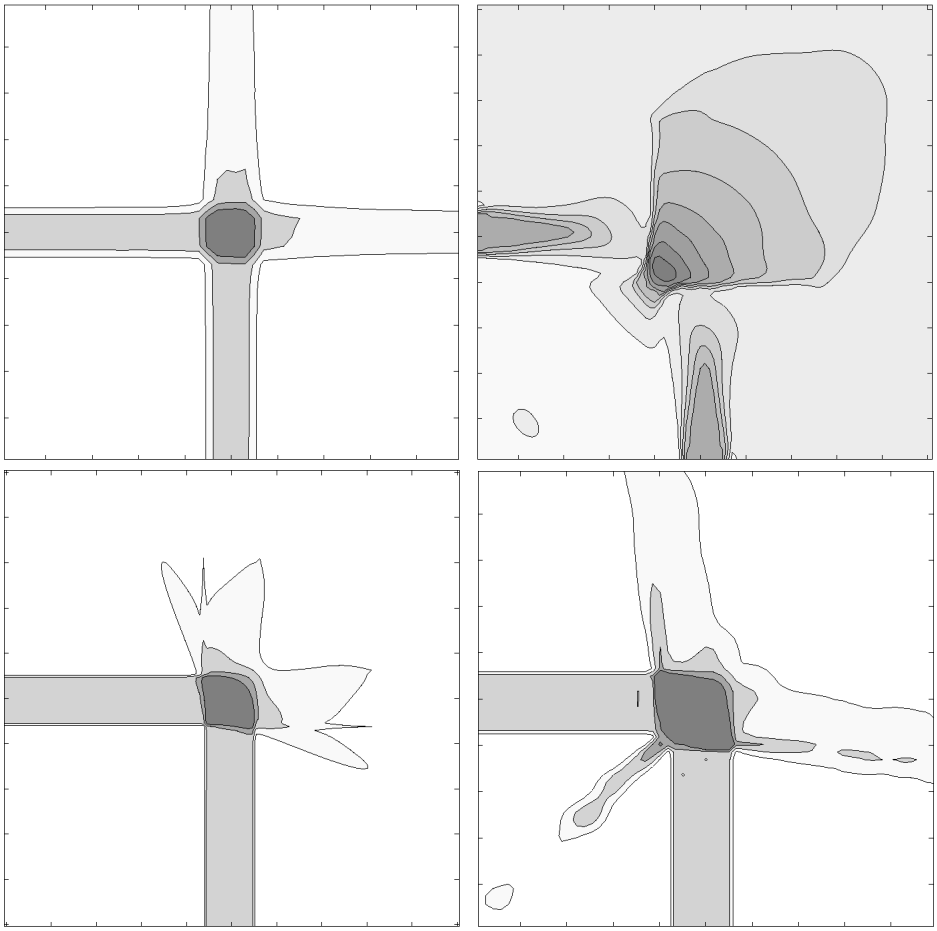

FIGURE 3. Particles' number density map and isocontours for crossing jets with $Kn = 1$. Density proportional to darkness. Domain size: 1 m $\times$1 m. Top left: Lagrangian. Top right: full second-order model. Bottom left: QMOM #1. Bottom right: QMOM #2.

5.2. *Taylor-Green flow*

The Taylor-Green flow consists of periodic vortices in cells with alternate rotating direction (figure 1). The fluid velocity is defined as follows:

$$V_{f,x} = \sin x \cos y$$
$$V_{f,y} = -\sin y \cos x$$

In this test case, particles are transported and experience drag. Different inertial regimes were explored, characterized by their Stokes number:

$$\mathrm{St} = \frac{\tau_p}{\tau_f} = \frac{2\rho_p r^2}{9\mu_f}.$$

τ_f, the fluid characteristic time, is 1 in this case due to domain size 1×1 m^2 and fluid maximum velocity 1 m/s. The main interest of this test case is the stationary state exhibited for $St = 1$ where a complex pattern in the particle spatial distribution is observed. For low inertia particles (e.g., $St = 0.1$), the particles quickly accumulate

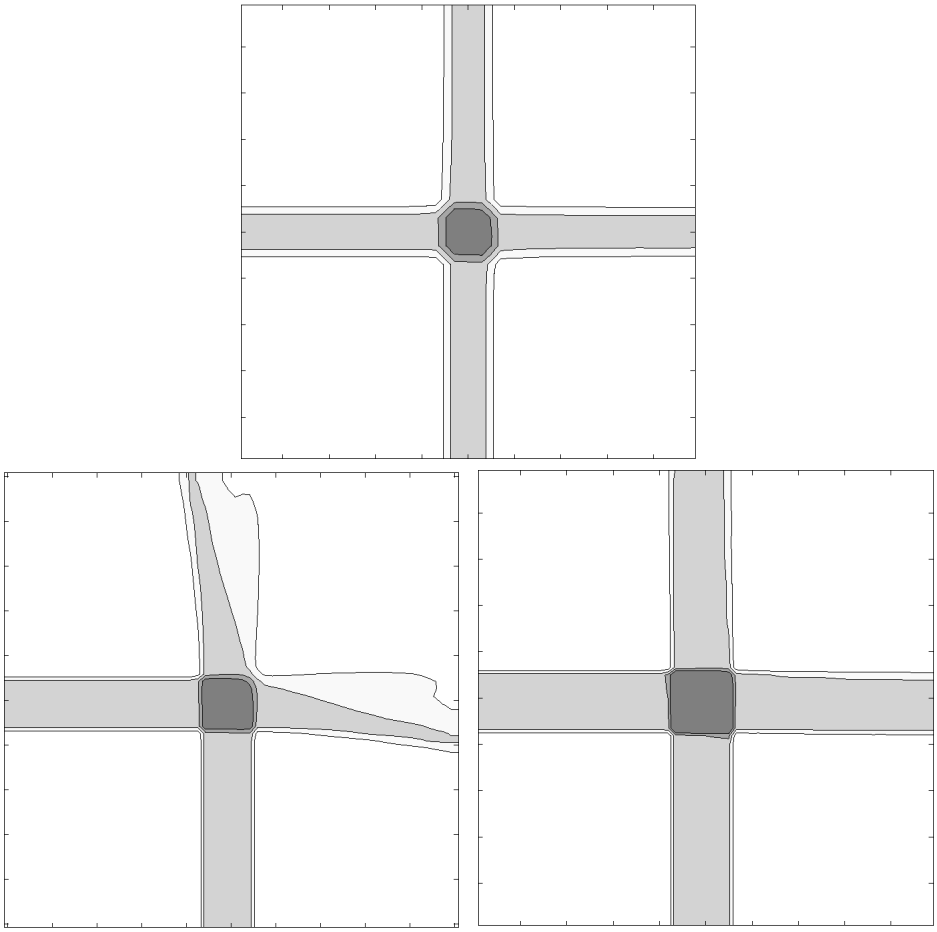

FIGURE 4. Particles' number density map and isocontours for crossing jets with $Kn = 5$. Density proportional to darkness. Domain size: 1 m $\times$1 m. Top left: Lagrangian. Top right: full second-order model. Bottom left: QMOM #1. Bottom right: QMOM #2.

at the nodes of the cells whereas for large inertia particles (e.g., $St = 10$) the spatial distribution has no stationary state. These last two behaviors are predicted by the two quadrature methods.

Results for $St = 1$ are shown in Fig. 5. The full second-order model predicts the presence of low-density areas centered on the vortices, but particles also accumulate in areas that are empty in the Lagrangian result. The quadrature methods' predictions of empty areas compared to the Lagrangian results are much better, but there are lines of high particle density that are not observed in the Lagrangian results.

6. Conclusions

Our evaluation of the results of the quadrature methods compared to a kinetic stress transport model is encouraging, with noticeable qualitative improvement when the particle velocity distribution is far from equilibrium. For the crossing jets, the quadrature-based moment methods get results closer to the Lagrangian results when collisions de-

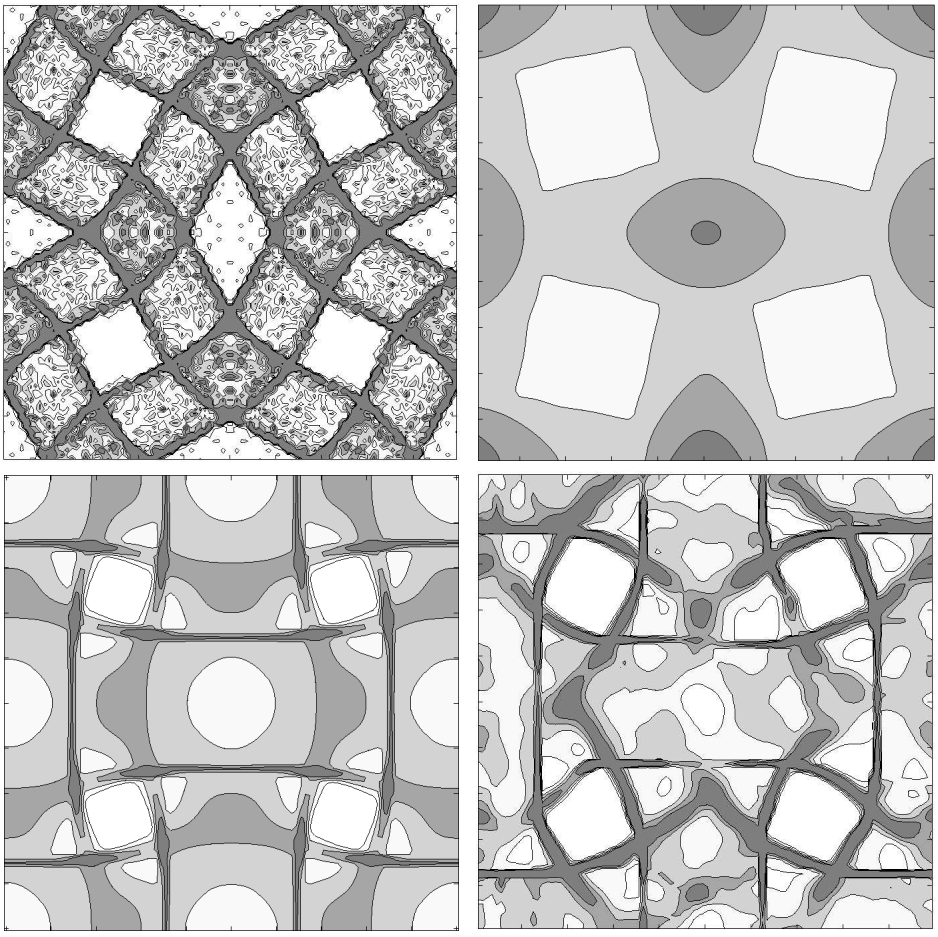

FIGURE 5. Particles' number density map and isocontours for Taylor-Green flow, stationary state, $St = 1$. Density proportional to darkness. Domain size: 1 m×1 m. Top left: Lagrangian. Top right: full second-order model. Bottom left: QMOM #1. Bottom right: QMOM #2.

crease, and the results (not presented here) are identical in the no-collision limit. In the $St = 1$ Taylor-Green flow, where particle trajectory crossing is important as can be seen from the Lagrangian result, the velocity distribution is far from equilibrium, and features of the Lagrangian particle spatial distribution are much better predicted by quadrature-based methods than the kinetic stress tranport model.

Overall, in many instances, the Eulerian results are significantly different from those of the Lagrangian method. However, the quadrature-based methods can be improved by going up in order of the transported moments, at the cost of a slightly increased computational time. For isotropic homogeneous turbulence flow, a great qualitative improvement of the results as compared to a first-order model has been demonstrated using a more basic quadrature method than the two described here (Desjardins, Fox & Villedieu

2008). Hence, in low collisional turbulent flows, we expect the quadrature-based moment methods to give better results than existing moment method.

REFERENCES

Babovsky, H. 1986 On a simulation scheme for the Boltzmann equation. *Math. Med. Appl. Sc.* **8**, 223–233

Bhatnagar, P. L., Gross, E. P. & Krook, M. 1954 A Model for Collision Processes in Gases. I. Small Amplitude Processes in Charged and Neutral One-Component Systems. *Phyical Review* **94**, 511–525

Chapman, S. & Cowling, T. G. 1970 *The Mathematical Theory of Non-Uniform Gases.* Cambridge University Press, Cambridge, England

Desjardins, O., Fox, R. O. & Villedieu, P. 2008 A quadrature-based moment method for dilute fluid-particle flows. *Journal of Computational Physics* **227**, 2514–2539

Fevrier, P., Simonin, O. & Squires, K. 2005 Partitioning of particle velocities in gas-solid turbulent flows into a continuous field and a spatially uncorrelated random distribution: theoretical formalism and numerical study. *Journal of Fluid Mechanics* **533**, 1–46

Fox, R. O. 2008 A quadrature-based third-order moment method for dilute gas-particle flows. *Journal of Computational Physics* **227**, 6313–6350

He, J. & Simonin, O. 1993 Non-equilibrium prediction of the particle-phase stress tensor in vertical pneumatic conveying. *Gas-Solid Flows-1993, ASME FED*, **166**, 253–263

McGraw, R. 1997 Description of aerosol dynamics by the quadrature method of moments. *Aerosol Science and Technology* **27**, 255–265

Nanbu, H. K. 1980 Direct simulation scheme derived from the Boltzmann equation. I. Monocomponent gas. *J. Phys. Soc. Jap.* **49**, 2042–2049

Sakiz, M. & Simonin, O. 1999 Numerical experiments and modelling of non-equilibrium effects in dilute granular flows. *Rarefied Gas Dynamics, Proceedings of the Twenty-First International Symposium on Rarefied Gas Dynamics, July 1998, Marseille, France*, Cépaduès Editions, **1**, 287–294

Simonin, O. 1991 Prediction of the dispersed phase turbulence in particle-laden jets. *Gas-Solid Flows-1991, ASME FED*, **121**, 197–206